Nandan A K[1], Aneesh Mathew[2], Padala Raja Shekar[3]

Trend Analysis of Aerosol Concentrations over Last Two Decades from MODIS Retrievals over Hyderabad District of India

Abstract: Air pollution is one of the grave concerns of the modern era, claiming millions of lives and adversely impacting the economy. Aerosols have been observed to play a significant role in negatively influencing climatological variables and human health in given areas. The current study aimed to study the trend of aerosols and particulates on daily, monthly, seasonal, and annual levels using a 20-year (2002–2021) daily mean aerosol optical depth (AOD) product released by moderate resolution imaging spectrometer (MODIS) sensors for the Hyderabad district in India. The results of the daily mean analysis revealed a rising trend in the number of days with severe AOD (>1), whereas examinations of the seasonal and monthly mean data from 2017 through 2022 showed that peak AOD values alternated between the summer, autumn, and winter seasons over the years. Trend analysis using Mann–Kendall, modified Mann–Kendall, and innovative trend analysis (ITA) tests revealed that AOD increased significantly from 2002 through 2021 ($p < 0.05$; $Z > 0$). Furthermore, correlation analysis was performed to check for correlations between AOD levels and certain meteorological factors for the Charminar and Secunderabad regions; it was noticed that temperature had a weak positive correlation with AOD ($p < 0.05$; $r = 0.283$ [Secunderabad] – $p < 0.05$; $r = 0.301$ [Charminar]), whereas relative humidity developed a very weak negative correlation with AOD ($p < 0.05$; $r = -0.079$ [Secunderabad] – $p < 0.05$; $r = -0.109$ [Charminar]).

Keywords: aerosol pollution, aerosol optical depth, trend analysis, correlation, meteorological variables

[1] National Institute of Technology, Department of Civil Engineering, Tiruchirappalli, Tamil Nadu, India, https://orcid.org/0009-0005-0147-5790

[2] National Institute of Technology, Department of Civil Engineering, Tiruchirappalli, Tamil Nadu, India, email: aneesh52006@gmail.com, aneesh@nitt.edu (corresponding author), https://orcid.org/0000-0001-6185-2360

[3] National Institute of Technology, Department of Civil Engineering, Tiruchirappalli, Tamil Nadu, India, https://orcid.org/0000-0001-5697-7329

1. Introduction

Air pollution has become a serious threat to humankind, posing numerous health risks (particularly in developing countries like India). The unprecedented growth in pollution can be attributed to various natural and anthropogenic sources such as automobiles, household combustion devices, industrial facilities, and forest fires. Although the growth of large-scale industries and services propels a country's economic development, they also play a part in the gradual decline of air quality – particularly in urban areas [1]. Over the years, air pollution has become a prominent contributor to the global burden of diseases. In 2019, the World Health Organization (WHO) estimated that about 99% of the world's population resided in areas that did not meet the organization's standards for air quality. The WHO estimated that, in 2019, ambient air pollution was solely responsible for more than 4.2 million premature deaths globally – 89% of which occurred in low- and middle-income countries. In the case of India, the number of premature deaths was estimated to be around 1.67 million in 2019, making up 17.8% of all of the deaths in the country [1].

The Environment Protection Agency (EPA) has designated six pollutants as "criteria" air pollutants, including carbon monoxide, lead, nitrogen oxides, ground-level ozone, sulfur oxides, and particulate matter. These pollutants should be taken into consideration while researching the features of air pollution. They were designated as criteria pollutants because the EPA controls them by creating health- and environment-based standards for figuring out their permitted limits in ambient air. One of these pollutants has recently been identified as having a significant detrimental impact on both human health and the climate – particulate matter (PM) [2, 3]. Particulates are categorized as PM_{10} (for those with diameters that are equal to or below 10 μm) and $PM_{2.5}$ (for those with diameters that are equal to or below 2.5 μm). Long-term exposure to $PM_{2.5}$ has been linked to increased risks of bronchitis, lung disease, and mortality, while acute exposure can irritate eyes, noses, and throats [4]. For epidemiological investigations, it is essential to obtain accurate estimates of $PM_{2.5}$ particulates at a high spatiotemporal resolution due to its devastating consequences for humans [5]. Numerous ground-based monitoring stations have been constructed worldwide to address this demand; however, these stations suffer from lower spatial resolution and discontinuous spatial coverage due to their sparse distribution (which makes the data that they produce unreliable). Studies have suggested that this limitation can be overcome by supplementing the ground-based data with global aerosol observation data from sources such as satellites (which have a broader spatial coverage) [4, 6].

The definition of aerosols is that they are the suspensions of small particles of solids (like dust and particulate matter) and liquids (like water droplets) in an air medium [7, 8]. Natural sources of aerosols involve seas (which release sea salt), deserts (which pollute the air with fine sand particles), wildfires, and volcanoes (both releasing smoke and ash into the atmosphere). On the other hand, anthropogenic sources mainly consist of traffic, industries, the construction sector, and household

emissions in urban areas, whereas biomass-burning and various farming activities form the bulk of the emissions from rural areas [9, 10]. Studies have shown that aerosols can affect the Earth's overall radiation budget by scattering or absorbing incoming solar radiation depending on their physical and chemical properties [11, 12]. The radiative effect of aerosols can also negatively affect the amount of precipitation over a region, as the interception of solar radiation by aerosols results in a decrease in the amount of insolation that reaches the ground surface; this, in turn, develops a shortage of sufficient heat energy for evaporating water and activating convective rain clouds 13]. In addition to their radiative effect, aerosols also play an active role in cloud formation. Zhang et al. [14] found that the number of aerosol particles has a significant impact on shaping the microphysical characters of clouds.

Several studies investigated the correlation between $PM_{2.5}$ concentrations and aerosols, and many of them established a linear correlation between the two variables [7]. However, there are some limitations to this relationship. While $PM_{2.5}$ particles consist solely of fine dry solid particles, AOD is influenced by water vapor and coarser particles [15]. A study that was performed by Tariq et al. [16] used AOD data from MODIS, MISR, and sea-viewing wide field-of-view sensors as well as meteorological and vegetation index data to analyze the long-term trends, followed by AOD and its linkage with vegetation and climatic variables in South-Asia. The correlation analysis showed a positive correlation between AOD and relative humidity ($r > 0.54$) in parts of Pakistan and central India as well as a negative correlation in most of the other regions. Moreover, a negative correlation ($r = -0.3$) was reported between AOD and the vegetation index in eastern Pakistan and western India.

Wang et al. [17] investigated the trend that was followed by aerosols in Taiwan from 2003 through 2019 using daily MAIAC AOD data with a one-kilometer resolution. The temporal analysis of AOD resulted in a decreasing trend over the study period. Tan et al. [18] used AOD data from the Himawari-8 satellite to study the spatio-temporal variations of AOD over Japan. Spatial analysis revealed that AOD showed higher values in the Seto Inland Sea region. Khalid et al. [19] studied and compared the variations in AOD on monthly and seasonal scales over the eastern and western routes of the China-Pakistan Economic Corridor using MODIS and MISR satellite data sets. It could be observed from the results that the MODIS AOD values followed a decreasing trend in the summer season for both routes, whereas no such trend was reported in the case of the MISR values. A study that was performed by Luong et al. [20] compared the variation that had been undergone by AOD and $PM_{2.5}$ on seasonal scales in Hanoi, Vietnam, in 2016. While both AOD and $PM_{2.5}$ levels recorded dips during the summer, $PM_{2.5}$ showed increases during the other seasons; on the other hand, AOD marked a reduction in the spring, followed by an increase in the winter.

Abuelgasim et al. [21] analyzed the long-term trends of aerosols over the United Arab Emirates (UAE) using the daily MODIS AOD product for the period of 2003–2018. It could be observed that the AOD values peaked during the spring

and summer months, which the authors attributed to the sandstorms that affect-ed the region during this period. Yousefi et al. [22] carried out the first long-term study on the AOD trend in Iran using data sets that were retrieved from MODIS and MERRA-2 instruments as well as the MODIS-MERRA-2 merged-data set. An analysis on a spatial scale revealed that the AOD values showed an increasing trend toward southwestern Iran, whereas the trend declined in the cases of lands at high altitudes in the northern and western regions. A study that was performed by Mohammad et al. [8] used Mann–Kendall and Sen's slope-estimator methods to investigate the trend that was followed by AOD over 18 years in Jharkhand, India. A spatial analysis of the AOD data revealed that the highest value could be found in the northeastern part of the state (which is subjected to large-scale mining activities and industrial emissions), whereas the southwestern part showed the lowest value. Gouda et al. [23] used AOD data from the MODIS sensor on the Terra satellite to investigate the drop in AOD over India during the COVID-19 lockdown period. In India, the northern region has a 22.53% reduction in AOD levels, whereas the south-ern region has a significantly smaller drop (approx. −0.31%), likely due to continued anthropogenic activity during the lockdown time.

A long-term pan-Indian trend analysis of AOD was performed by Kumar [24] using 20-year data that was retrieved from the MODIS sensor. It could be observed that the western longitudes near Rajasthan showed relatively high AOD values (around 0.85) when compared to the eastern longitudes during the monsoon months; this was attributed to the high wind speeds over Rajasthan that, in turn, were capa-ble of increasing the aerosol concentrations by producing jet droplets and spumes. Singh et al. [25] examined the climatological trends in AOD over the urban and rural areas of the Indo-Gangetic Plain using data that was retrieved from the MODIS sen-sors that were onboard the Terra and Aqua satellites. The frequency distribution of the monthly data revealed that the AOD values were higher (as high as 1.35) in the rural area during October for both the Aqua and Terra data.

India was ranked fifth in the list of the most-polluted countries by the WHO in 2019 based on the amount of $PM_{2.5}$ emissions; moreover, 21 of the top 30 polluted cities were situated in India [26]. These figures are enough to understand the gravity of the air pollution in India. High levels of pollution (especially particulate matter) have been significantly contributing to the figures of disease burden and mortality for over a decade. This situation calls for the need to develop trends for these pol-lutants so as to analyze the pollution scenario in India and devise appropriate strat-egies and long-term solutions to minimize this threat. After a thorough review of the literature, some gaps were identified in the research. Though some studies per-formed trend analyses on long-term aerosol data using conventional Mann–Kendall and Sen's slope methods, very few have employed advanced methods that are ca-pable of handling auto-correlations and outliers in the data sets (such as modified Mann–Kendall or innovative trend analysis in trend detection). The current study makes novel attempts to investigate long-term trends in aerosols using advanced

trend-analysis techniques (which have also not been performed thus far in the Indian scenario).

Aerosol concentrations are changing the climatic picture of each region. As a result, it is critical to comprehend the long-term trends in aerosol concentrations as well as the variations that aerosols undergo on various spatial and temporal scales. To satisfy these desires, a variable that can quantitatively represent the aerosol-loading in the atmosphere must exist; this is where a variable called aerosol optical depth comes into play.

This study provides a pioneering investigation into the long-term trends of aerosols and particulate matter – specifically focusing on the Hyderabad district in India. The extended temporal analysis of two decades that utilized high-resolution MODIS sensor data stands as a unique contribution for understanding the evolution of the air quality parameters in this region. Furthermore, the integration of multiple advanced statistical techniques for trend analysis (including Mann–Kendall, modified Mann–Kendall, and innovative trend analysis [ITA]) sets a new benchmark for robustly identifying and confirming the observed trends in aerosol levels. Additionally, the exploration of the seasonal variability in peak AOD values over the years brings forth a novel perspective on the complex dynamics of aerosol distribution across different climatic seasons, shedding light on previously unexamined patterns in the area's air quality. Encompassing both temporal and seasonal dimensions, this study's comprehensive approach offers a unique lens for comprehending the intricate interplay between aerosols and meteorological factors as well as their implications for human health and regional climate dynamics in Hyderabad.

Air pollutants (particularly aerosols) not only hurt human health but also have an impact on climate phenomena. According to [13], aerosols have a significant impact on both surface temperature fluctuations and the suppression of precipitation in a given area. As a result, creating aerosol-prediction models and researching long-term patterns in aerosol concentrations are crucial. These elements served as inspirations for the formulation of three study objectives, which are covered in the next section. The objectives of this study were as follows:

- analyze time series data of AOD and study daily, monthly, seasonal, and annual variations in aerosol concentration;
- identify significant long-term trends in aerosol concentration on different time scales by means of various trend-analysis methods;
- study relationship between AOD and various meteorological factors through correlation analysis.

2. Study Area

The Indian district of Hyderabad was chosen as the study area. The district is located between the longitudes of 78°38′ and 78°56′ East and the latitudes of 17°29′ and 17°48′ North. The district houses the city of Hyderabad, which is both the state

capital and the largest city in the state of Telangana. Hyderabad has been recognized as the fourth-most-populous city in India (with a population of about 9.7 million residents in the metropolitan region alone) according to the census data from 2011 [27].

Based on Köppen–Geiger classification, the climate of Hyderabad has been identified as 'BSh,' where 'B' indicates dry conditions, 'S' indicates a semi-arid climate, and 'h' stands for hot. In short, Hyderabad experiences a dry and hot semi-arid climate in general. However, the southwest monsoon brings heavy rainfall to Hyderabad between June and October (accounting for the majority of its annual rainfall). The city's mean annual temperature is 26.6°C, with monthly mean temperatures ranging from 21°C to 33°C. May is the hottest month (with temperatures reaching 36–39°C), while December and January have the coolest temperatures (ranging 14.5–28.0°C). Figure 1 shows a map of the Hyderabad district, along with maps of India and the state of Telangana.
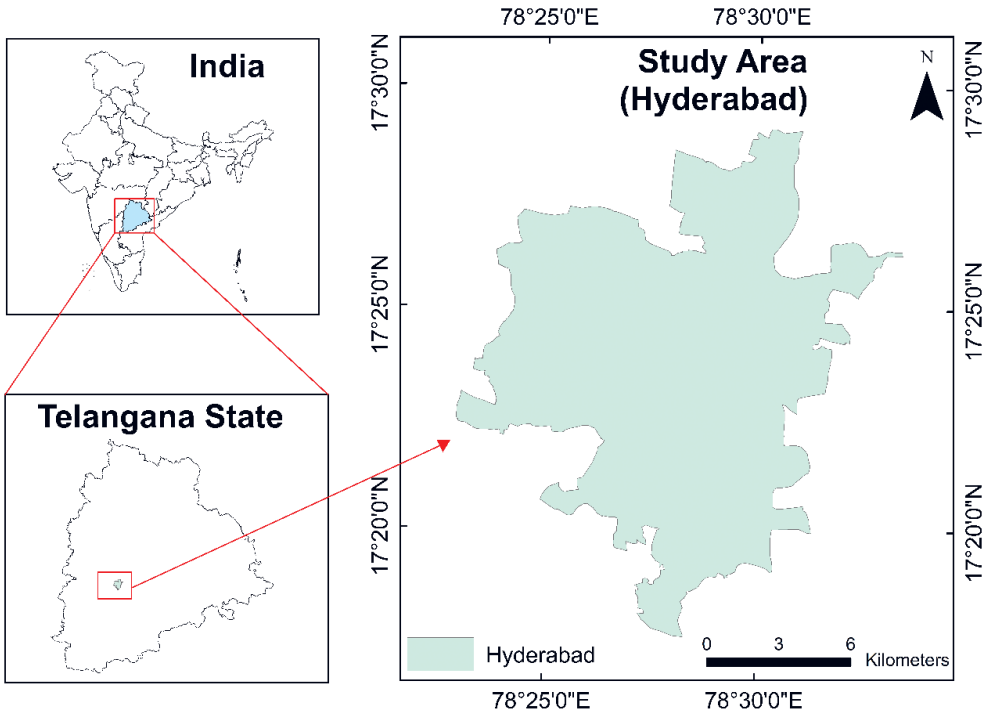

Fig. 1. Maps of study area

Hyderabad has four distinct seasons. Winter in Hyderabad lasts from December through February, followed by a hot summer period (from March through May). The monsoon season begins in June and lasts until September, while the autumn season encompasses the months of October and November. This seasonal classification has been adopted for the present study. Hyderabad is a rapidly growing city

that has witnessed a significant deterioration in ambient air quality over the last decade; this has been primarily due to increased traffic and the presence of industries in the outskirts of the northern and eastern parts of the city. Vehicle emissions are one of the most significant sources of pollution in Hyderabad, and the rising population density will only worsen the situation in the future. In 2022, the $PM_{2.5}$ concentration in Hyderabad was observed to be 15.2 times higher than the WHO's annual air quality guideline. Furthermore, air pollution alone is thought to have caused the deaths of around 12,000 people in Hyderabad through 2021. All of these facts make Hyderabad an important target for studies of air pollution.

3. Data and Methodology

This section explains the methodology that was chosen for the study as well as the ideas and guiding principles that underlay the various approaches that were used in the trend analysis and factor studies that were carried out in the current phase. Figure 2 shows the flow chart of the methodology.
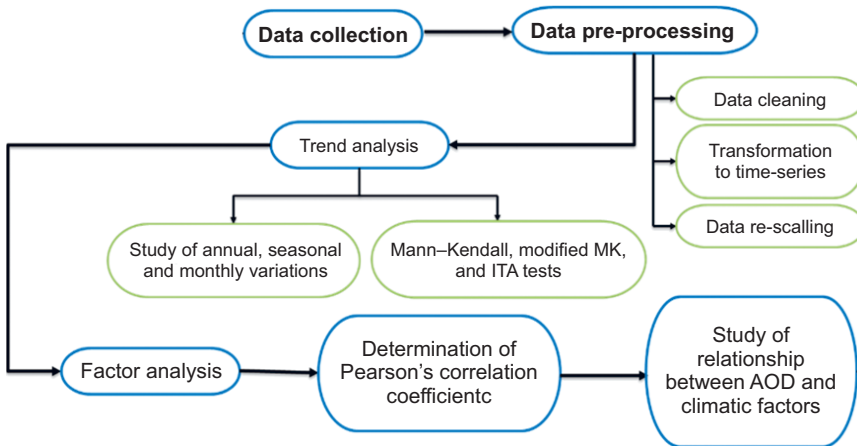

Fig. 2. Flow chart of methodology

The present study began with the collection of the required data of the aerosol optical depth (AOD), meteorological parameters, and $PM_{2.5}$ concentrations for the study area. The AOD data was pre-processed and prepared for analysis and modeling. Data pre-processing is a three-stage process that involves the following stages:
1. data cleaning (in which missing and erroneous values are checked for and removed),
2. transformation of raw data into time series,
3. re-scaling of data to obtain actual AOD values.

The AOD data that had already been cleaned up was then averaged on yearly, seasonal, and monthly bases. The variations that were experienced by AOD on these time scales during each year of the study period were compared and studied using the averaged data. The next stage of the study involved analyzing the long-term trends in the averaged data using the Mann–Kendall, modified Mann–Kendall, and innovative trend analysis (ITA) tests. The study was concluded with an investigation of the correlations between AOD and various meteorological parameters using Pearson's correlation coefficients in order to clarify the existence and type of relationship between the aerosol concentration and each of the parameters.

4. Data Collection

The data set that was used involved AOD values and meteorological data for the Hyderabad district over the time period of January 2002 through February 2021. The daily mean AOD data was extracted from the MCD19A2 product data (which consisted of a combination of data with a one-kilometer resolution that was retrieved from the MODIS sensors aboard the Terra and Aqua satellites) processed through the multi-angle implementation of atmospheric correction (MAIAC) algorithm to minimize the interference of the clouds and surface reflectance on the AOD values. Out of the 13 datasets that were offered in the MCD19A2 product, the green band with a wavelength of 0.55 μm was used in the study, as green bands are commonly used as standards in AOD models and for AOD validation [28]. The fully processed ready-made data set was retrieved by running the relevant codes in Google Earth Engine.

The meteorological parameters that were required for the study were extracted from the POWER Data Access Viewer web mapping application offered by NASA (National Aeronautics and Space Administration). For the sake of the correlation studies, daily average data was collected for two locations in the Hyderabad district; namely, Secundarabad and Charminar. The various parameters for which the data was obtained are listed in Table 1, along with their annotations and measurement units.

Table 1. Meteorological parameters collected for study

Parameter	Annotations	Unit
Relative humidity	RH	%
Rainfall	RF	mm
Temperature	T	°C
Wind speed	WS	m/s
Wind direction	WD	degree

Despite the data sets that are described above, the current phase of the study also required the total fire-count data in and around the study area from 2016 through 2022. This information was obtained from NASA's Fire Information for Resource Management System (FIRMS) portal.

5. Data Pre-Processing

The data-collection process was succeeded by data pre-processing. The entire processes that were involved in the pre-processing were performed using the 'pandas' and 'numpy' libraries of the Python programming language. The data was initially checked for null or missing values that could have resulted from the cloud-masking and atmospheric-correction processes of the MAIAC algorithm. These values were removed from the data set. Furthermore, the data was also checked and cleaned for any outliers that may have arisen due to faulty detection or reading. Similar to AOD, the meteorological data was also checked for missing values and outliers.

The next stage of the pre-processing involved obtaining the daily mean AOD values from the multiple data sources for a single day in order to transform the raw AOD data into a proper time series. The AOD data that was obtained had its values exaggerated by a factor of 1000; therefore, re-scaling was performed on the dataset to retrieve the actual AOD values for the study area.

6. Trend Analysis

Trend analysis forms an important objective of the study during the first phase. The AOD data that was averaged over the monthly, seasonal, and annual scales would serve as inputs for three different tests:
5) Mann–Kendall and Sen's slope-estimator test,
6) modified Mann–Kendall test,
7) innovative trend analysis (ITA).

The current section focuses on the concepts that underlay each of the tests as well as the variables and conditions that were involved.

6.1. Mann–Kendall and Sen's Slope-Estimator Test

The Mann–Kendall test is generally applied for analyzing time-series information for persistently increasing or decreasing trends. The advantage of this method is that it works independently from the distribution of the data; i.e., it does not require the input data to strictly follow any distribution [8]. Therefore, this test can be described as a non-parametric test.

The goal of the test is to determine whether an assumption (known as a null hypothesis) should be accepted or rejected. For trend tests, a null hypothesis indicates that there is no significant trend in the data.

For a given set of data, the test starts with determining the sign of the difference between each data point and all of the data points that succeeds it pairwise. This information shall be used to estimate a parameter known as S [8] by using the relationship that is given in Equation (1):

$$S = \sum_{i=1}^{n-1} \sum_{j=i+1}^{n} \text{sgn}(y_j - y_i) \tag{1}$$

where n is the number of observations, y_j is the jth observation, y_i is the ith observation, and sgn(.) is a function that is computed [8] by using Equation (2):

$$\text{sgn}(y_j - y_i) = \begin{cases} +1, & \text{if } (x_j - x_i > 0) \\ 0, & \text{if } (x_j - x_i = 0) \\ -1, & \text{if } (x_j - x_i < 0) \end{cases} \tag{2}$$

In short, S calculates the difference between all of the upward and downward trends among the data. The mean and variance of the S statistic [8] are given in Equations (3) and (4), respectively:

$$E(S) = 0 \tag{3}$$

$$\text{var}(S) = \frac{1}{18} \left[n(n-1)(2n+5) - \sum_{p=1}^{q} t_p(t_p - 1)(2t_p + 5) \right] \tag{4}$$

When calculating the variance, the second term deals with the elimination of the variance due to the tied (or equal) values in the data. The term q is the number of tied groups, each having t_p observations.

Using the S statistic and its variance, the Mann–Kendall Z value [8] shall be calculated by using the relationship that is shown in Equation (5):

$$Z = \begin{cases} \dfrac{S-1}{\sqrt{\text{var}(S)}}, & \text{if } S > 0 \\ 0, & \text{if } S = 0 \\ \dfrac{S+1}{\sqrt{\text{var}(S)}}, & \text{if } S < 0 \end{cases} \tag{5}$$

The data trend can be reported as an increasing trend for a positive Z value and a decreasing trend for a negative Z value; if the value of Z is 0, it is safe to assume that there is no trend in the data. The monotonicity (or significance) of the trend can be identified by using another statistical parameter known as the p-value, which is

the confidence limit for the test. A p-value that is obtained in a test is compared with a predefined parameter (known as confidence level 'α') to conclude the significance of the trend if the p-value is less than α. The confidence level is usually set to values like 0.10, 0.05, and 0.01. In practice, using a 5% (0.05) level of significance has become common practice [29].

If the results of Mann–Kendall test show a trend, the rate of the change of the trend can be calculated by using Sen's slope-estimator test [30], as is shown in Equation (6):

$$d_k = \text{median}\left(\frac{x_j - x_i}{j - i}\right) \tag{6}$$

It is evident from the equation that Sen's slope-estimator test calculates the median value of all of the slopes between each pair of data points in a data set.

6.2. Modified Mann–Kendall Test

The Mann–Kendall test is an efficient tool for detecting trends in a sample; however, the presence of serial autocorrelation in the sample will affect the performance of the test, leading to the reporting of false trends. To account for the issue of autocorrelation, a correction parameter that is known as effective sample size (n^*) is utilized [31, 32]. The effective sample size can be computed by using Equation (7):

$$\frac{1}{n^*} = \frac{1}{n} + \frac{2}{n^2}\sum_{j=1}^{n-1}(n-j)\big(\rho(j)\big) \tag{7}$$

Here, n is the actual sample size, while $\rho(j)$ is known as the auto-correlation function (which accounts for the correlation among the sample). The effective sample size value is used to update the variance of the Mann–Kendall S statistic in order to obtain a corrected variance [31], as is shown in Equation (8):

$$\text{corrected var}(S) = \text{var}(S)\cdot\frac{n}{n^*} \tag{8}$$

This variance is used to compute the corrected value of Z by using Equation (5). The rest of the procedure is similar to what was discussed for the Mann–Kendall test.

6.3. Innovative Trend Analysis (ITA) Test

Şen [33] proposed ITA as a graphical trend-analysis test for detecting trends and sub-trends in time series data. Aside from autocorrelation, the method can also handle outliers [34]. The step-by-step procedure for constructing an ITA graph is described in the flow chart that is shown in Figure 3.
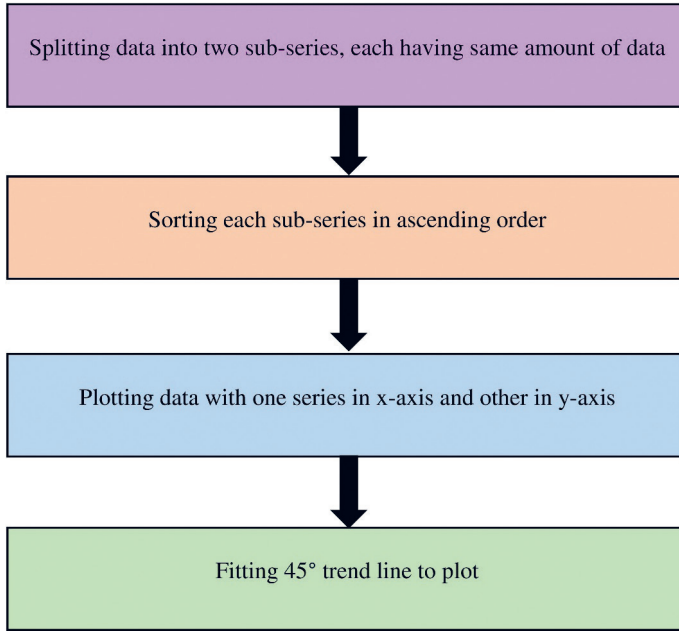
Fig. 3. Procedure of ITA

As described in the flow diagram, the ITA method requires the data to be split into two sub-series with equal numbers of observations. If the number of observations is odd, one of the data points can be considered to be an outlier and is removed from the data set. Each of the resulting sub-series shall be sorted in ascending order and would be plotted against each other. A 45° trend line shall then be fitted onto the data set. If the scatter points are clustered above the trend line, the trend can be reported as increasing; otherwise, the trend is decreasing. If the scatter lies along the trend, it can be inferred that the time series follows no trend [34].

The monotonicity of the trend can be checked by examining the locations of the scatter points concerning the trend line. If all of the scatter points lie on one side of the trend line, the trend can be reported as monotonic, whereas the distribution of the scatter points on either side of the trend line indicates a non-monotonic trend [33].

The slope of ITA [33, 34] can be computed using Equation (9):

$$B = \frac{1}{n}\sum_{i=1}^{n}\frac{10(x_j - x_i)}{\mathrm{mean}(x_i)} \tag{9}$$

where n is the number of observations in each sub-series, and x_j and x_i are the values of each consecutive sub-series. The null hypothesis assumed for the test (there is no slope) will be rejected if the computed slope angle is greater than the critical value that is determined using the standard deviation of the ITA slope.

7. Correlation Analysis

The present study was also devoted to analyzing the correlation between AOD and the various meteorological factors that may have influenced the aerosol concentration in the study area. Correlation studies are used to evaluate the relationship between two variables, wherein one is the predictor variable and the other the response variable. This can be performed by examining the strength of the statistical correlation between them. The direction and strength of the correlation between two factors can be analyzed using various correlation coefficients. However, when the variables are normally distributed and are measured on a continuous scale, Pearson's correlation coefficient (denoted as r) gives the appropriate results [36]. One limitation of Pearson's coefficient is that the presence of outliers in the data significantly affects the results [35].

For a pair of variables, coefficient r [36] can be calculated using Equation (10):

$$r = \frac{\text{cov}(X, Y)}{s_x s_y} \tag{10}$$

where $\text{cov}(X, Y)$ is the covariance between the normally distributed X and Y variables, with standard deviations s_x and s_y. The covariance can be computed [36] as shown in Equation (11):

$$\text{cov}(X,Y) = \frac{\sum_{i=1}^{n}(x_i - x')(y_i - y')}{n-1} \tag{11}$$

where x and y are the means of variables X and Y, respectively, and n is the number of observations.

Coefficient r can take up any value within a range of −1 to +1. A positive value for r is indicative of a positive correlation, whereas a negative value indicates a negative correlation. Table 2 shows the various ranges for the absolute value of the coefficient for which the coefficient can be reported from being very weak to very strong [37].

Table 2. Correlation strength based on r value

Absolute value of r	Correlation strength
0.0–0.2	very weak
0.2–0.4	weak
0.4–0.6	medium
0.6–0.8	strong
0.8–1.0	very strong

Furthermore, the statistical significance of the obtained correlations can be determined using the p-value. In this case, the p-value represents the likelihood that the correlation between two variables happened by chance. P-values that are less than the significance level (usually 0.05) can be marked as being significant [29].

8. Results and Discussion

The AOD data that was collected was pre-processed in order to obtain the daily mean AOD for a period of 20 years (2002–2022). The data was analyzed for variations on daily, yearly, seasonal, and monthly time scales. In addition, a long-term trend analysis was performed on the monthly, seasonal, and yearly mean time-series in order to identify any significant trends. Finally, correlation analysis was performed on the data sets of AOD and the collected meteorological variables in order to study the correlation between AOD and each of the meteorological parameters.

9. Daily, Yearly, Season-Wise, and Month-Wise AOD Variations

The daily mean data for 20 years was used to determine the number of days for which AOD exceeded 1 for each year. It was assumed that an AOD value that was greater than 1 was a severe case. Figure 4 shows the result of the analysis of the AOD trend for the last two decades.
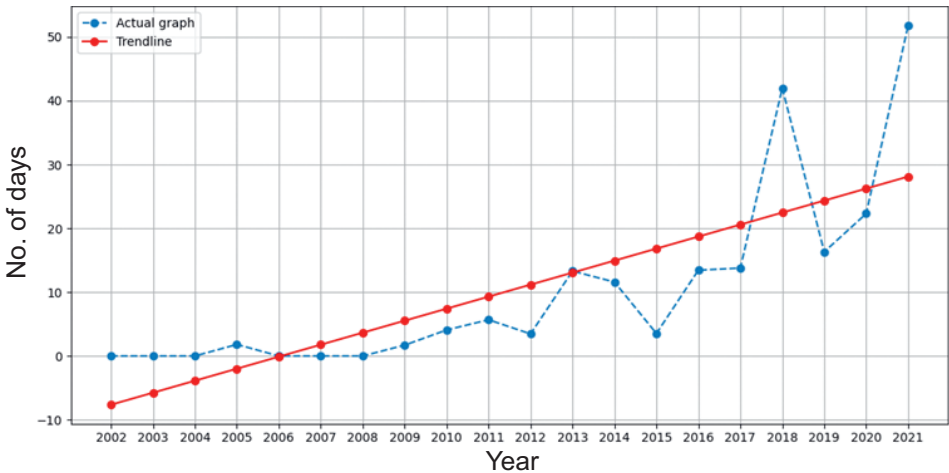

Fig. 4. Numbers of days with severe AOD values

It can be understood from Figure 4 that, even though the number of days with severe AOD did not follow a consistently increasing pattern year after year, there

was a general trend of an increase in the number of severe days (as is depicted by the shown trendline). Moreover, a drastic increase could be observed in the numbers of severe days in 2018 (42 days) and 2021 (52 days). This could be attributed to the increase in the pollution due to the anthropogenic activities and industrial emissions over the recent years.

The daily mean data was then averaged on a yearly basis and was then analyzed for variation over 20 years. The results of this analysis are shown in Figure 5.
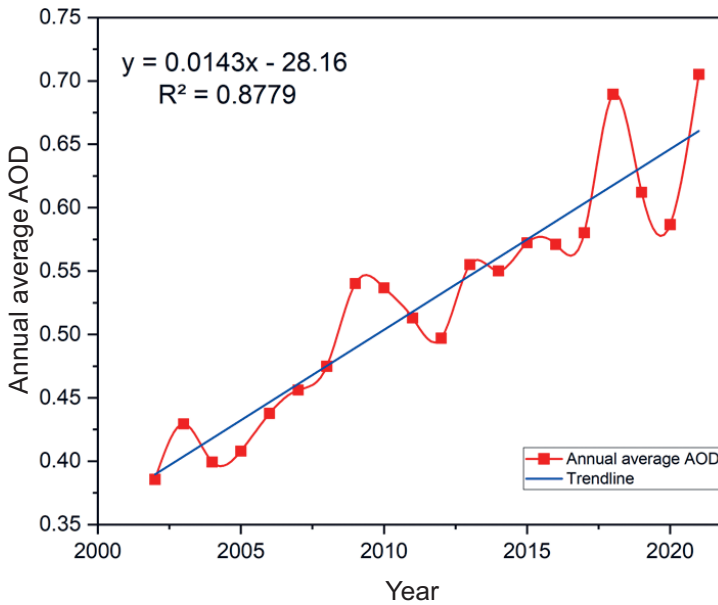

Fig. 5. Annual average AOD distribution (2002–2021)

It can be observed from the trendline that the yearly mean AOD followed a general increasing trend over the 20-year period, undergoing an increase by 45.31% and with sharp spikes at 2018 (mean AOD = 0.6895) and 2021 (mean AOD = 0.7052). A comparison of Figures 4 and 5 shows that the annual average AOD distribution followed an almost similar pattern as the distribution of the number of severe AOD days.

An analysis was also conducted on a seasonal scale for the AOD data. Hyderabad is considered to experience four seasons – winter (December through February), summer (March through May), monsoon (June through September), and autumn (October through November). An analysis of the 20-year-long seasonal mean AOD data from 2002 through 2021 showed that the AOD values recorded an increase of 48.77% for the winter seasons across the timespan, whereas the autumns saw an increase of 46.96%. While the summers' mean AOD underwent a rise of 44.61%, the monsoon seasons' reported the lowest growth (38.39%) over the years. In spite of the general trend calculation, a detailed analysis and comparison were

carried out on the season-wise distribution of AOD for a five-year period (from 2017 through 2021) using box plots. The results of the analysis have been reproduced in Figure 6.
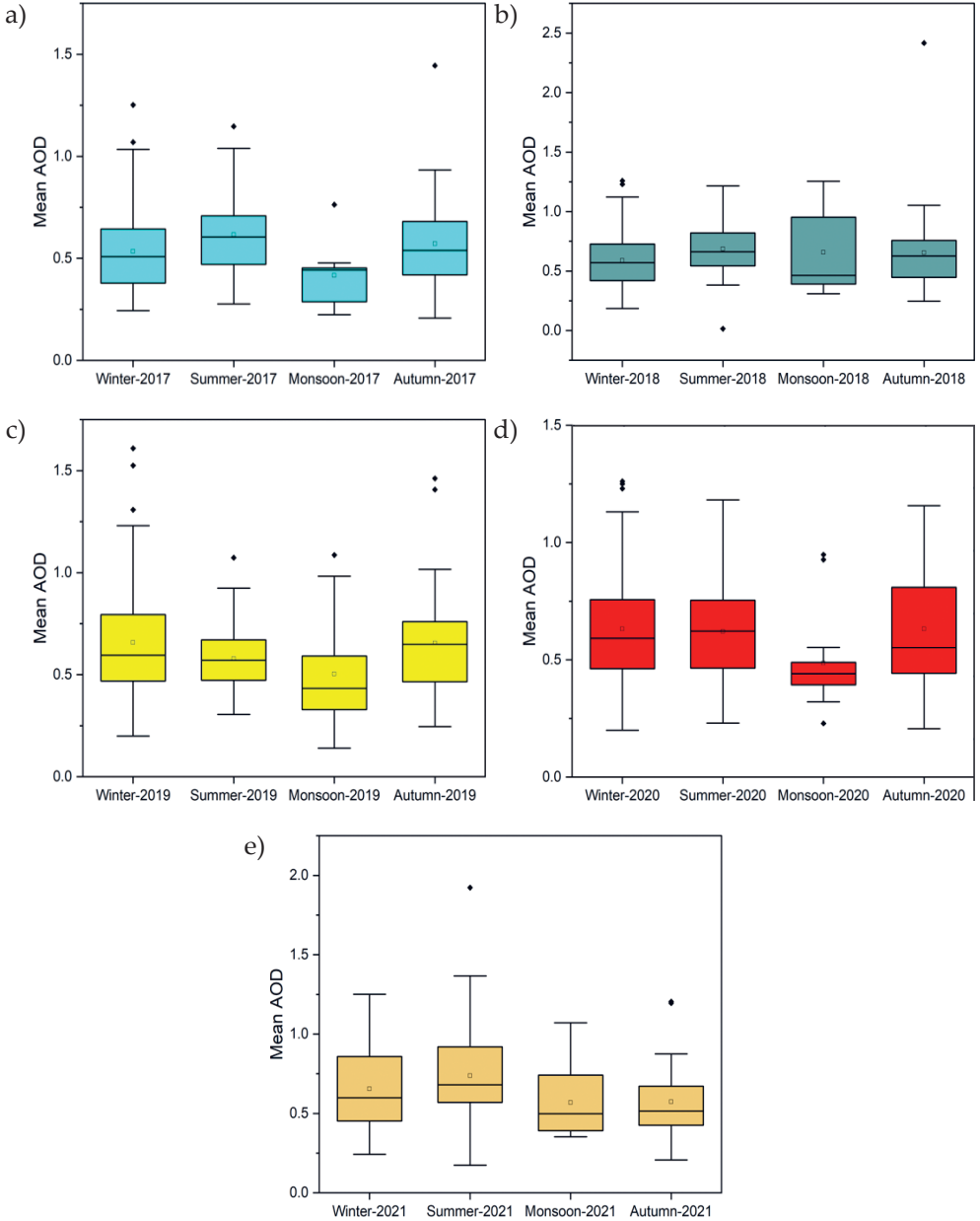

Fig. 6. Seasonal data-distribution of AOD: a) 2017; b) 2018; c) 2019; d) 2020; e) 2021

Figure 6 displays the season-wise distribution of AOD during the five years from 2017 through 2021. The AOD values were found to vary over a range that extended from 0.015 to 2.416 in general. It could be observed that the monsoon seasons recorded the lowest AOD mean value (approx. 0.5) during the study period. This might be a consequence of the washout of aerosols during the rainfall monsoon period as well as the lack of data from the months of the monsoon due to cloud formations [38]. It was also noticed that the greatest levels of the mean AOD values were recorded during the summer seasons for the years of 2017 (0.61), 2018 (0.7), and 2021 (0.73). A study that was conducted by David et al. [39] pointed out that westerly winds cause the transportation of mineral dust from the Arabian and Thar deserts toward the Indian subcontinent during the summer seasons. While this phenomenon could be a contributor to the aerosol loading over Hyderabad, there was another region-specific cause that might significantly contribute to the aerosol loading. The state of Telangana (where Hyderabad is situated) is prone to forest fires during the summer months. A further study was conducted using six-year (2016–2021) fire-count data from NASA's FIRMS portal for a territory that was comprised of the Hyderabad district and those regions that were located within two pixels from the district boundary in all directions. The results of the study (which involves a comparison of the fire count [factored by 100 for convenience] and the summer mean AOD) have been reproduced in Figure 7.
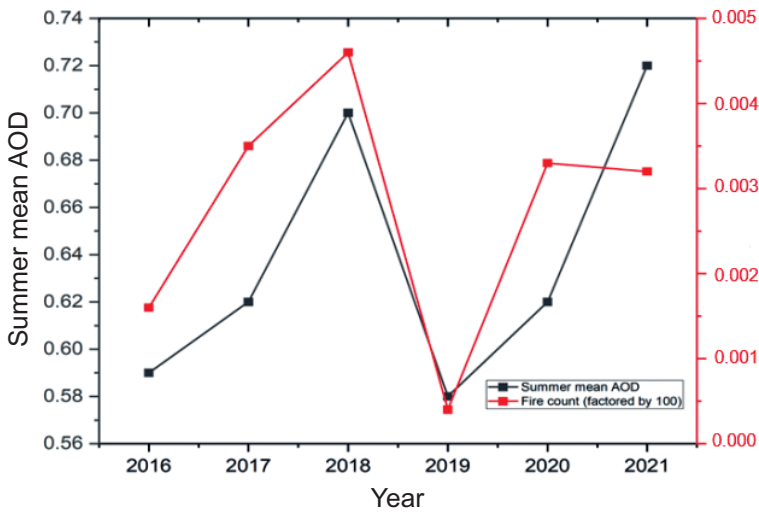

Fig. 7. Comparison of fire count and summer mean AOD

It is evident from Figure 7 that the fire count and AOD followed a similar pattern over the years (with the exception of 2021). While both the fire count and AOD registered increases during the period of 2016 through 2018 and in 2020, both of the values experienced sharp dips in 2019. The 91.3% drop in the fire count in 2019

(as compared to 2018) was accompanied by a 21% drop in AOD for the same year. However, contrasting patterns could be observed in 2021; it was discovered upon our investigation that, even though the fire count dipped in 2021 (as compared to 2020), the fire incidents in 2021 occurred closer to the study region when compared to the other years. Because of this fact, more smoke might have concentrated in the study region in that year, causing the rise in AOD. The biomass plumes that were generated by the fires were transported by northerly winds toward Hyderabad (as was observed in a study by Attri et al. [40]).

It was also found from the seasonal analysis of 2019 and 2020 that the AOD values showed higher mean values in the autumn (AOD = 0.73 in 2019) and winter (AOD = 0.65 in 2020) seasons than in the other seasons. These could have been attributed to the increases in aerosol loading as a result of various anthropogenic activities [39] as well as to the phenomenon of inversion, which typically blocks the vertical dispersion of aerosols higher into the atmosphere in the winter months [41].

Finally, the AOD values were also analyzed for variations on a monthly scale for a five-year period (2017–2021); the results from this analysis are shown in Figure 8.

Figure 8 shows the month-wise distribution of AOD in the forms of boxplots during each of the years from 2017 through 2021. Similar to the seasonal distribution, the monthly AOD values were also observed to fall within a range that stretched from 0.015 to 2.416 during the study period.

It could be observed from the analysis of the plots that the month of October recorded the maximum mean AOD values in both 2017 (AOD = 0.694) and 2020 (AOD = 0.889), while November recorded the highest level in 2019 (AOD = 0.751) and December recorded the highest level in 2018 (AOD = 0.893). Interestingly, April displayed the highest value in 2021 (AOD = 0.793); however, the second-highest value for the year (which was recorded in January – AOD = 0.775) differed by only 2.26% from the value from April. Therefore, it was evident from the observations that Hyderabad experienced relatively higher mean aerosol concentrations during the months of the autumn and winter seasons for the past five years. A study that was performed by Sinha et al. [42] identified the supremacy of fine-mode aerosols, which usually originate as a result of such human activities as fossil fuel combustion and manure burning during the winter season. The extent and intensity of these activities would only increase over time with increasing populations and demands for resources, thereby becoming eminent contributors to the aerosol loading during the winter months over the years. Interestingly, the higher mean values in the autumn season can also be attributed to the fine-mode aerosols that might have either been generated locally or transported by northerly winds from the northern parts of India (where kharif crops are burnt in bulk amounts during the months of October and November [42].

Sinha et al. [42] also found that the cases with AOD levels that were lower than 0.4 during March to May could have been related to the presence of coarse-mode aerosols due to the transport of mineral dust toward Hyderabad, whereas the

higher AOD values could have been attributed to the fine-mode aerosols that were developed as a result of the gas-to-particle conversion that was caused by the strong insolation and forest fires (as discussed earlier).
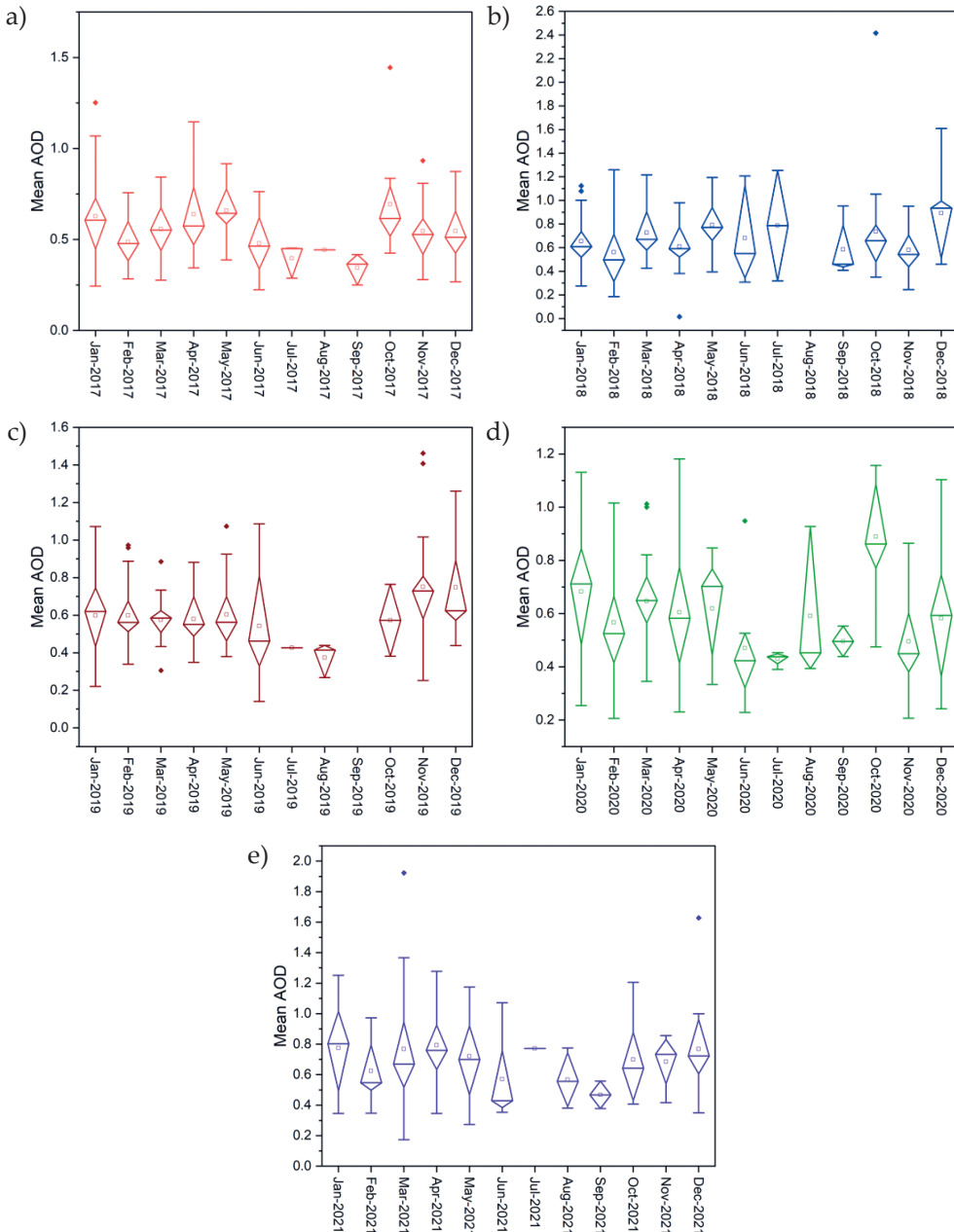

Fig. 8. Month-wise distribution of mean AOD: a) 2017; b) 2018; c) 2019; d) 2020; e) 2021

An observation of the boxplots during the summer months of March, April, and May showed that the AOD values were above 0.4 on most of the days during these months. This was evident from the analysis of the first quartile values, which were found to be greater than 0.4 during these months for all of the years (with their minimum value of 0.421 occurring during April 2019). Therefore, it can be said that AOD acquired values that were below 0.4 for fewer than 25% of the days during the summer months. Correlating these observations with the findings of Sinha et al. [42], it can be concluded that the aerosol loading in Hyderabad for more than a quarter of the days in the summer months during the period of 2017 through 2022 could have been ascribed to the releases from the forest fires and gas conversions.

On the other hand, a comparison of the AOD means showed that, with the exception of 2018, the minimum mean values were recorded by the months in the monsoon season (July 2020 [AOD = 0.430], August 2019 [AOD = 0.374], September 2017 [AOD = 0.344], and September 2021 [AOD = 0.468]). As an exception, February reported the lowest mean of all of the months in 2018 (AOD = 0.562), only to be followed by September (AOD = 0.585) at a margin of 3.93%. However, it was evident from the plots that the AOD values spanned across a very narrow range of values for most of the monsoon months, with some months showing only one value (or none at all). This was due to the unavailability of data for many days during the monsoon months (possibly due to cloud obstruction). Owing to this, the variations that pertained to the monsoon period that were discussed above might not have been able to provide an accurate picture of the real aerosol distribution in the study area.

10. Trend Analysis over Hyderabad District

The long-term trends of AOD were analyzed on 20-year AOD data on monthly, seasonal, and annual timescales using the Mann–Kendall and Sen's slope-estimator, modified Mann–Kendall, and innovative trend analysis tests. The results of the tests form the essence of this section.

10.1. Mann–Kendall and Sen's Slope-Estimator Test

The common practice of adopting 0.05 as the significance level has been adopted in the current study. The null hypothesis that was assumed for the study is that the time series shows no significant trend. The test was performed using the 'trend' package of the R programming language. The results of the test are presented in Table 3.

It could be observed from the test that the AOD values followed a positive (increasing) trend on the monthly, seasonal, and annual timescales, as Mann–Kendall Z reported positive values in all of the cases. In addition, the p-values were observed to fall much below the significance limit of 0.05, thereby indicating that all of the observed trends were statistically significant. Therefore, it can be concluded that AOD followed a statistically significant increasing trend (denoted by Δ in Table 3) on all of the time scales.

Table 3. Results of Mann–Kendall test

Period	p	Mann–Kendall S	Variance of S	Mann–Kendall Z	Trend	Sen's slope
January	5E-06	142.00	950.00	4.57	Δ	0.020
February	9E-05	122.00	950.00	3.93	Δ	0.013
March	1E-04	120.00	950.00	3.86	Δ	0.016
April	3E-06	144.00	950.00	4.64	Δ	0.012
May	3E-05	130.00	950.00	4.19	Δ	0.012
June	7E-03	84.00	950.00	2.69	Δ	0.009
July	1E-04	118.00	950.00	3.80	Δ	0.016
August	8E-04	104.00	950.00	3.34	Δ	0.012
September	7E-04	105.00	949.00	3.38	Δ	0.012
October	2E-05	134.00	950.00	4.32	Δ	0.018
November	5E-05	126.00	950.00	4.06	Δ	0.014
December	3E-06	146.00	950.00	4.70	Δ	0.017
Winter	0E+00	149.00	817.00	5.18	Δ	0.017
Summer	4E-05	128.00	950.00	4.12	Δ	0.013
Monsoon	2E-05	132.00	950.00	4.25	Δ	0.012
Autumn	1E-06	152.00	950.00	4.90	Δ	0.015
Annual	0E+00	164.00	950.00	5.29	Δ	0.014

Additionally, Table 3 displays the Sen's slope values for each data set. The slopes of all of the data sets were generally positive, indicating a rising trend (as was previously determined by the Z-statistic). The highest Sen's slope value was recorded in January (slope = 0.020) and was 55% greater than the lowest Sen's slope value which was recorded for June (slope = 0.009) according to a comparison of the slopes for each month.

Sen's slope values varied somewhat among the seasons, with winter having the highest slope (slope = 0.017) and the monsoon season having the lowest (slope = 0.012) according to an analysis of the seasonal Sen's slope values. For the yearly case, the Sen's slope value was found to be 0.014.

10.2. Modified Mann–Kendall Test

The time series data was also subjected to the modified Mann–Kendall test, wherein the problem of autocorrelation among the data was accounted for and corrected using various measures. A significance level of 0.05 was assumed for the test.

As in the case of the Mann–Kendall test, a null hypothesis of no trend was assumed for this test, The modified Mann–Kendall test was performed using the 'modifedmk' package of the R programming language. The results of the test have been reproduced in Table 4.

Table 4. Results of modified Mann–Kendall test

Period	New p-value	n/n^*	New variance	Corrected Z	Trend
January	8.00E-18	0.283	269.09	8.5955	Δ
February	5.00E-25	0.144	137.15	10.332	Δ
March	2.00E-34	0.099	94.81	12.221	Δ
April	2.00E-23	0.217	206.44	9.953	Δ
May	3.00E-19	0.218	207.62	8.953	Δ
June	8.00E-10	0.192	182.74	6.139	Δ
July	7.00E-40	0.082	78.39	13.215	Δ
August	2.00E-29	0.088	83.75	11.255	Δ
September	4.00E-17	0.16	152.26	8.428	Δ
October	7.00E-30	0.144	137.31	11.35	Δ
November	1.00E-18	0.213	202.22	8.79	Δ
December	3.00E-12	0.452	429.65	6.995	Δ
Winter	9.00E-29	0.216	176.67	11.135	Δ
Summer	1.00E-21	0.185	176.08	9.571	Δ
Monsoon	5.00E-33	0.126	119.59	11.979	Δ
Autumn	2.00E-54	0.099	94.64	15.521	Δ
Annual	1.00E-66	0.094	89.21	17.257	Δ

It could be observed from the results that the Mann–Kendall Z value achieved positive values on all of the timescales (even after being corrected for autocorrelation). This was indicative of the presence of increasing trends for all of the data sets.

Similarly, the modified p-value test attained values that were well below the significance limit of 0.05 in all cases, thereby proving that all of the observed trends were statistically significant. Therefore, the results of the modified Mann–Kendall test also showed a statistically significant increasing trend (denoted by Δ in Table 4) on all of the timescales.

10.3. Innovative Trend Analysis (ITA) Test

The last phase of the trend analysis dealt with the innovative trend analysis test on the time series data. ITA is a graphical test wherein the autocorrelations and outliers in the data would be accounted for during the analysis. The necessary procedure for obtaining the required graphs were followed, and the obtained results are displayed in Figures 9–11.
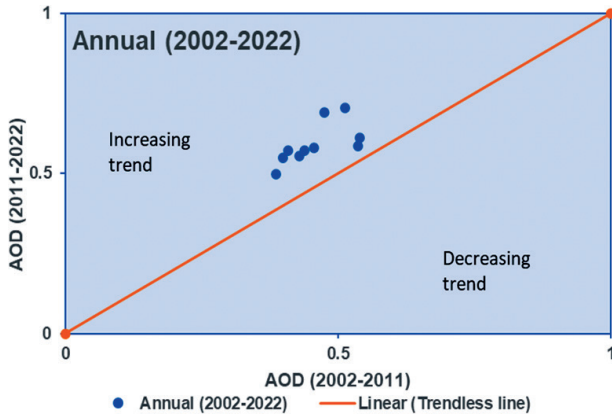

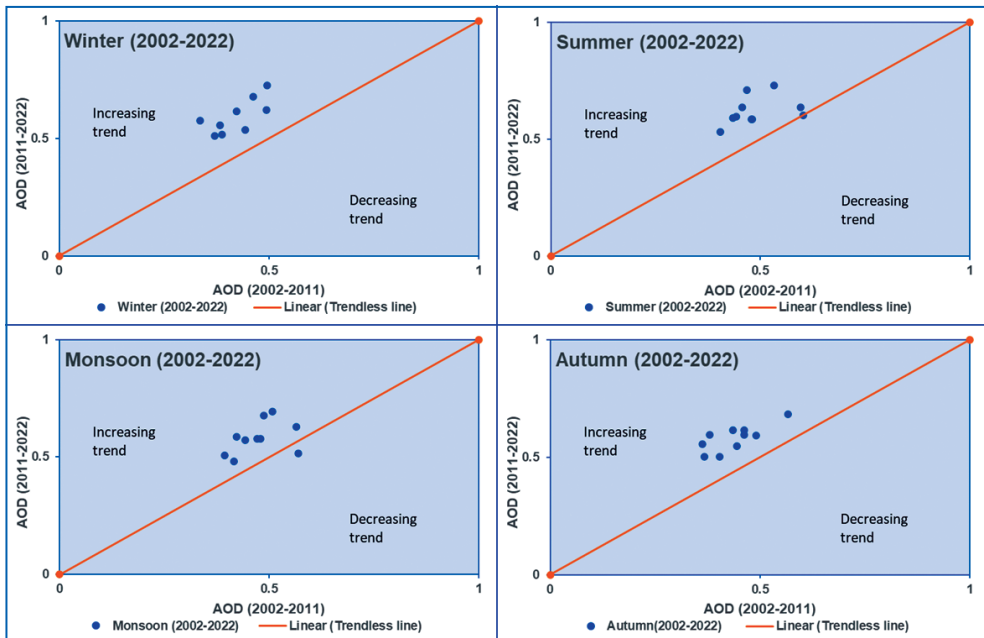**Fig. 9.** ITA graph for annual timeseries data

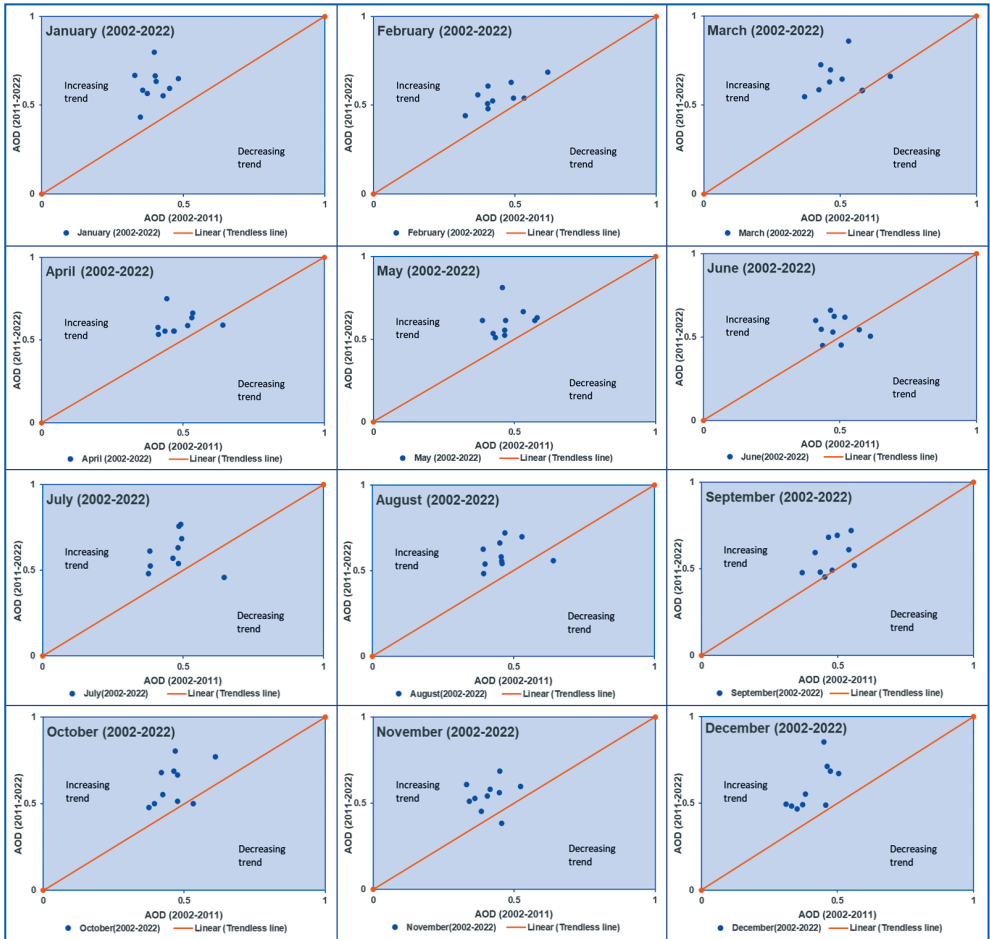**Fig. 10.** ITA graphs for seasonal timeseries data

Fig. 11. ITA graphs for monthly timeseries data

From the results, it was noted that a major cluster of data points was located above the line of no trend for each of the cases, which indicates that AOD followed an increasing trend on the monthly, seasonal, and yearly timeframes.

The significance of the trends was analyzed by finding the slopes of the ITA trends and comparing them with the 95-percent confidence-limit values that were obtained from the standard deviations of these slopes. The results of the analysis are presented in Table 5. The results showed that the ITA lopes attained values that were greater than the absolute critical value at a 95% confidence limit, thereby proving that all of the obtained trends were statistically significant.

The monotonicity of the trends was also checked using the ITA plots. It was found that the months of January–March, May, and December, all of the seasons except for the monsoon season, and the annual time series followed strictly monotonic

trends that increased. Among the non-monotonic trends (except for June), all of the other time series showed weak non-monotonicity, as only one scatter point could be observed to fall below the trend line in all of the cases. Hence, it can be concluded from the results of the three trend-analysis tests that the AOD values followed significantly increasing trends in all of the timeframes over a 20-year period (2002–2022).

Table 5. Results of significance test

Period	Slope of ITA	Std. deviation of slope	Absolute critical value
January	0.022	0.001	0.002
February	0.011	0.000	0.001
March	0.015	0.001	0.002
April	0.011	0.001	0.001
May	0.013	0.001	0.002
June	0.006	0.001	0.001
July	0.013	0.001	0.003
August	0.013	0.001	0.002
September	0.009	0.001	0.001
October	0.015	0.001	0.002
November	0.013	0.001	0.001
December	0.018	0.001	0.003
Winter	0.015	0.001	0.001
Summer	0.013	0.000	0.001
Monsoon	0.011	0.000	0.001
Autumn	0.014	0.000	0.001
Annual	0.013	0.001	0.001

11. Correlation Analysis

A correlation analysis was carried out using the 20-year daily mean data for AOD and various meteorological factors that are listed in Table 6; these were checked for correlation by measuring Pearson's correlation coefficient (r). In order to check for spatial variability in the correlation, a study was performed on the data from two urban locations in the northern and southern territories of Hyderabad; namely, Secunderabad and Charminar.

Statistical descriptions of the factors that were considered in the study are shown in Tables 6 and 7.

Table 6. Descriptive statistics of meteorological variables in Secunderabad

| Factor	Annotations	Unit	Mean	Std. deviation	Min. value	Max. value
AOD	AOD	–	0.42	0.17	0.02	1.31
Rainfall	RF	mm	0.32	1.94	0	60.17
Wind speed	WS	m/s	3.31	0.87	1.16	8.32
Wind direction	WD	degree	133.58	67.6	15.38	343.88
Temperature	T	°C	25.7	4.77	16.07	36.93
Relative humidity	RH	%	48.73	17.58	8.56	89.38

Table 7. Descriptive statistics of meteorological variables in Charminar

Factor	Annotations	Unit	Mean	Std. deviation	Min. value	Max. value
AOD	AOD	–	0.43	0.18	0.01	1.81
Rainfall	RF	mm	0.33	1.98	0	60.17
Wind speed	WS	m/s	3.31	0.88	0.97	7.94
Wind direction	WD	degree	135.41	67.52	15.38	343.88
Temperature	T	°C	25.87	4.80	16.07	36.93
Relative humidity	RH	%	48.13	17.42	8.56	89.50

The correlations among the various factors are presented in Figures 12 and 13. It could be observed from the correlation plots that there were negligible spatial variations in the correlations among all of the factors except for the AOD/wind speed pair, which showed a significant weak negative correlation at Charminar (p-value ≤ 0.05; $r = -0.08$); this correlation was absent in the Secunderabad data.

A significant weak positive correlation could be observed between AOD and temperature at both locations (p-value ≤ 0.05; $r = 0.283$ for Secunderabad/ p-value ≤ 0.05; $r = 0.301$ for Charminar). The positive relationships can be attributed to the presence of higher amounts of aerosols in the study areas – especially the black carbon (BC) that was released by forest fires and biomass burning [43] and transported by westerly winds in the summer months (as explained in the discussion on seasonal variations).
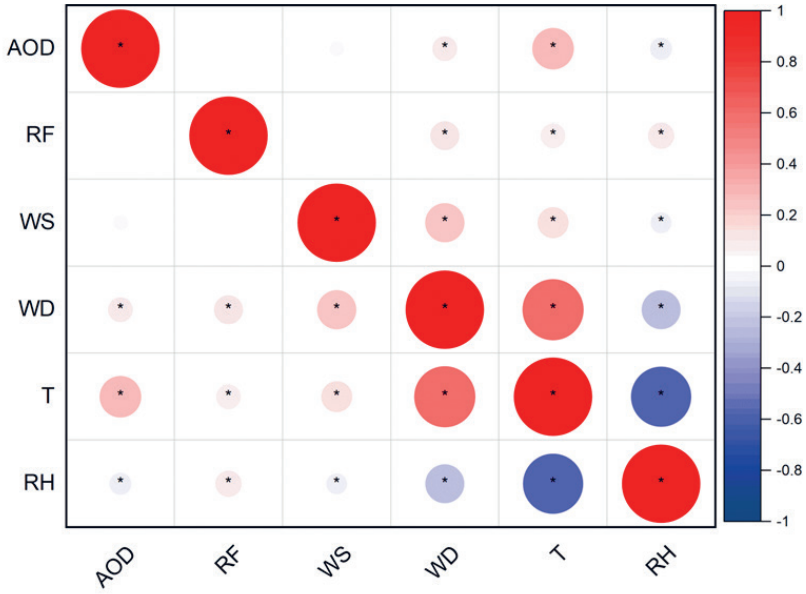
* *p* ≤ 0.05

Fig. 12. Correlation plot for Secunderabad
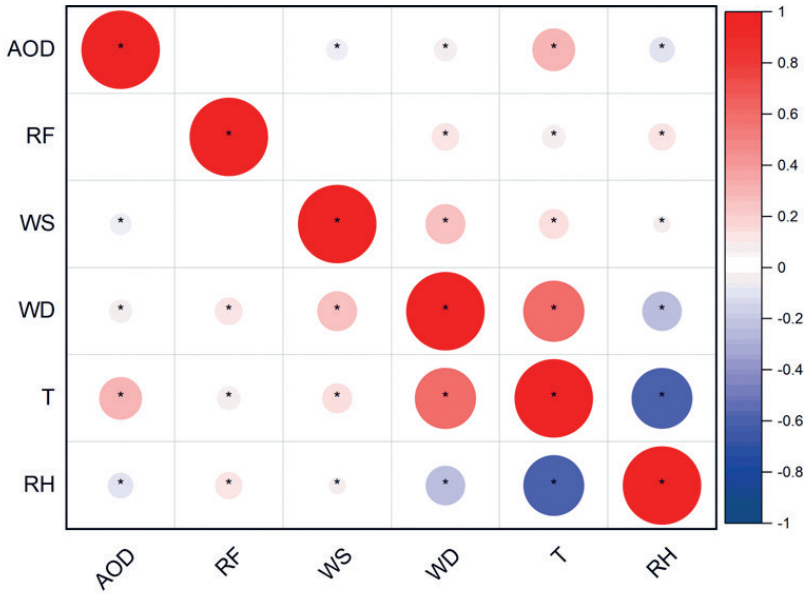
* *p* ≤ 0.05

Fig. 13. Correlation plot for Charminar

Relative humidity showed a very weak negative correlation with AOD (p-value ≤ 0.05; $r = -0.079$ for Secunderabad/ p-value ≤ 0.05; $r = -0.109$ for Charminar). Moreover, humidity was negatively related to temperature ($p \leq 0.05$; $r = -0.591$ for Secunderabad/ p-value ≤ 0.05; $r = -0.601$ for Charminar); therefore, it could be understood that humidity was higher during the winter than it was in the summer, and AOD was higher in the summer (when the humidity was low) as compared to the winter. Again, the negative correlation can be attributed to the accumulation of dust from fires and dust transport during the summer months.

The novelty of this study lies in its extensive 20-year analysis (2002–2021) using MODIS sensors and focusing on aerosol and particulate-matter trends in Hyderabad, India. Leveraging the daily mean aerosol optical depth (AOD) data, the study offers a comprehensive view of the daily, monthly, seasonal, and annual variations in aerosol levels. Employing diverse statistical tests such as Mann–Kendall, modified Mann–Kendall, and innovative trend analysis (ITA) validates the significant increasing trend in AOD. Notably, the identification of alternating peak AOD values among the seasons (summer, autumn, and winter) unveiled previously unexplored seasonal variabilities. Additionally, correlating AOD with meteorological factors like temperature and relative humidity revealed nuanced associations, with temperature displaying a weak positive correlation and relative humidity showing a weak negative correlation with AOD for the Charminar and Secunderabad regions. This multidimensional analysis (spanning an extensive time frame and utilizing satellite-based data) contributes uniquely to understanding long-term aerosol dynamics and their interactions with meteorological parameters in this specific geographical area.

12. Conclusions

Over the course of 20 years (from 2002 through 2021), data on AOD and a variety of meteorological parameters was gathered and pre-processed in order to be used as input in the study. This included analyzing daily, seasonal, monthly, and annual variations in AOD as well as trends in AOD using the ITA, Mann–Kendall, and modified Mann–Kendall trend tests along with a correlation analysis in which the obtained meteorological and AOD data was compared for correlations.

The conclusions that can be drawn from the present study are as follows:

1. An analysis of daily mean AOD data for 20 years revealed that the number of days with severe AOD concentrations followed an increasing trend over the years, with a substantially higher number of severe days in 2018 (42 days) and 2021 (52 days).
2. The yearly mean AOD distribution followed an increasing trend during the period of 2002–2021, with a percentage increase of 45.31%.
3. The AOD values followed an increasing trend for all of the seasons during the study period. The values increased by 48.77, 44.61, 38.39, and 46.96% during the winter, summer, monsoon, and autumn seasons, respectively.

4. The season-wise studies for data from 2017 through 2022 showed that AOD peaked during the summer seasons of 2017, 2018, and 2021 (with mean values of 0.61, 0.70, and 0.73, respectively), whereas peaks could be observed for the autumn and winter seasons of 2019 and 2020 (with respective mean values of 0.73 and 0.65).

5. A graphical comparison of the summer mean AOD and fire count data from 2016 through 2021 confirmed the role of forest fires in the aerosol load in Hyderabad.

6. The trend analysis for the 20-year data using the Mann–Kendall and modified Mann–Kendall tests revealed the presence of significant increasing trends ($p < 0.05$ and $Z > 0$) of the monthly, seasonal, and annual levels.

7. The results of the graphical ITA test signaled the presence of increasing trends with statistical significance (slope of ITA > 95% confidence limit) on the monthly, seasonal, and annual scales.

8. A correlation analysis with AOD and meteorological parameters from Secunderabad and Charminar showed that AOD developed a significant weak positive correlation with temperature at both locations (p-value ≤ 0.05; $r = 0.283$ for Secunderabad/ p-value ≤ 0.05; $r = 0.301$ for Charminar).

9. Relative humidity was observed to show a very weak negative correlation with AOD at both locations (p-value ≤ 0.05; $r = -0.079$ for Secunderabad/ p-value ≤ 0.05; $r = -0.109$ for Charminar).

From the findings of the study, it could be observed that the aerosol concentrations in the Hyderabad district have increased significantly over the past two decades, with AOD showing significant ($p < 0.05$) and positive ($Z > 0$) trends in the monthly, seasonal, and annual scales on all of the trend-detection tests. The distribution of aerosols in Hyderabad during the summer and winter seasons did not vary significantly throughout each year, although peak mean monthly aerosol concentrations could be observed to alternately occur in the summer and winter months in consecutive years. It could also be observed that forest fires played a significant role in the elevated aerosol concentrations in Hyderabad during the summer periods. Furthermore, the meteorological factors were found to have a minor influence on the aerosol concentrations in the city, as was evidenced by their weak correlations with AOD.

The study's key findings present critical implications for understanding and addressing air pollution in Hyderabad. The substantial increase in AOD over the past two decades indicates a grave escalation in air pollution levels, necessitating urgent intervention strategies. The observed alternating peaks in aerosol concentrations during the summer and winter months coupled with the correlation between heightened aerosol levels and forest fires during the summers underline the influence of seasonal variations and environmental factors on air quality. Despite their weak correlations, the linkages between meteorological parameters (like temperature and

relative humidity) with AOD offer valuable insights into refining predictive models, thus aiding in the more-accurate forecasting of aerosol concentrations in the region. These findings not only emphasize the need for immediate actions to curb air pollution but also underscore the importance of nuanced policies that are tailored to seasonal variations and diverse pollution sources, thus ensuring effective public health safeguards and environmental protection measures for Hyderabad's residents. The findings of the study, which focused on an analysis of long-term trends in aerosols, can provide valuable insight into the changing patterns of air pollution in Hyderabad (which is a Tier-1 city). The identification of long-term shifts and variations in aerosol levels can aid researchers in correlating them with various human activities, natural phenomena, and climate variations. This knowledge not only improves our understanding of air quality but also helps policymakers in their efforts to mitigate the negative effects of air pollution on public health and the environment. The results of the correlation analysis that was presented in the study can help researchers identify significant input factors for developing forecast models for aerosol concentrations in the Hyderabad district.

References

[1] Pandey A., Brauer M., Cropper M.L., Balakrisnan K., Mathur P., Dey S. Turgulu B. et al.: *Health and economic impact of air pollution in the states of India: The Global Burden of Disease Study 2019*. The Lancet Planetary Health, vol. 5(10), 2021, pp. e25–e38. https://doi.org/10.1016/S2542-5196(20)30298-9.

[2] He Y., Gao Z., Guo T., Qu F., Liang D., Li D., Shi J., Shan B.: *Fine particulate matter associated mortality burden of lung cancer in Hebei Province, China.* Thoracic Cancer, vol. 9(7), 2018, pp. 820–826. https://doi.org/10.1111/1759-7714.12653.

[3] Mathew A., Gokul P.R., Raja Shekar P., Arunab K.S., Ghassan Abdo H., Almohamad H., Abdullah Al Dughairi A.: *Air quality analysis and PM2.5 modelling using machine learning techniques: A study of Hyderabad city in India.* Cogent Engineering, vol. 10(1), 2023, 2243743. https://doi.org/10.1080/23311916.2023.2243743.

[4] Raju L., Gandhimathi R., Mathew A., Ramesh S.T.: *Spatio-temporal modelling of particulate matter concentrations using satellite derived aerosol optical depth over coastal region of Chennai in India.* Ecological Informatics, vol. 69, 2022, 101681. https://doi.org/10.1016/j.ecoinf.2022.101681.

[5] Li L., Zhang J., Meng X., Fang Y., Ge Y., Wang J., Wang C., Wu J., Kan H.: *Estimation of $PM_{2.5}$ concentrations at a high spatiotemporal resolution using constrained mixed-effect bagging models with MAIAC aerosol optical depth.* Remote Sensing of Environment, vol. 217, 2018, pp. 573–586. https://doi.org/10.1016/j.rse.2018.09.001.

[6] Van Donkelaar A., Martin R.V., Brauer M.: *Global estimates of ambient fine particulate matter concentrations from satellite-based aerosol optical depth: development and application.* Environmental Health Perspectives, vol. 118(6), 2010, pp. 847–855. https://doi.org/10.1289/ehp.0901623.

[7] Ranjan A.K., Patra A.K., Gorai A.K.: *A review on estimation of particulate matter from satellite-based aerosol optical depth: Data, methods, and challenges.* Asia-Pacific Journal of Atmospheric Sciences, vol. 57, 2020, pp. 679–699. https://doi.org/10.1007/s13143-020-00215-0.

[8] Mohammad L., Mondal I., Bandyopadhyay J., Pham Q.B., Nguyen X.C., Dinh C.D., Al-Quraishi A.M.F.: *Assessment of spatio-temporal trends of satellite based aerosol optical depth using Mann–Kendall test and Sen's slope estimator model.* Geomatics, Natural Hazards and Risk, vol. 13(1), 2022, pp. 1270–1298. https://doi.org/10.1080/19475705.2022.2070552.

[9] Calvo A.I., Alves C., Castro A., Pont V., Vicente A.M., Fraile R.: *Research on aerosol sources and chemical composition: Past, current and emerging issues.* Atmospheric Research, vol. 120–121, 2013, pp. 1–28. https://doi.org/10.1016/j.atmosres.2012.09.021.

[10] Gokul P.R., Mathew A., Bhosale A., Nair A.T.: *Spatio-temporal air quality analysis and $PM_{2.5}$ prediction over Hyderabad City, India using artificial intelligence techniques.* Ecological Informatics, vol. 76, 2023, 102067. https://doi.org/10.1016/j.ecoinf.2023.102067.

[11] Taneja K., Ahmad S., Ahmad K., Attri S.: *Time series analysis of aerosol optical depth over New Delhi using Box–Jenkins ARIMA modeling approach.* Atmospheric Pollution Research, vol. 7(4), 2016, pp. 585–596. https://doi.org/10.1016/j.apr.2016.02.004.

[12] Myhre G., Lund Myhre C.E., Samset B.H., Storelvmo T.: *Aerosols and their relation to global climate and climate sensitivity.* Nature Education Knowledge, vol. 4(5), 2013, 7.

[13] Rosenfeld D., Lohmann U., Raga G.B., O'Dowd C.D., Kulmala M., Fuzzi S., Reisell A., Andrae M.O.: *Flood or drought: How do aerosols affect precipitation?* Science, vol. 321(5894), 2008, pp. 1309–1313. https://doi.org/10.1126/science.1160606.

[14] Zhang Q., Quan J., Tie X., Huang M., Ma X.: *Impact of aerosol particles on cloud formation: Aircraft measurements in China.* Atmospheric Environment, vol. 45(3), 2011, pp. 665-672. https://doi.org/10.1016/j.atmosenv.2010.10.025.

[15] Yang Q., Yuan Q., Yue L., Li T., Shen H., Zhang L.: *The relationships between PM$_{2.5}$ and aerosol optical depth (AOD) in mainland China: About and behind spatio-temporal variations*. Environmental Pollution, vol. 248, 2019, pp. 526–535. https://doi.org/10.1016/j.envpol.2019.02.071.

[16] Tariq S., Qayyum F., Ul-Haq Z., Mehmood U.: *Long-term spatiotemporal trends in aerosol optical depth and its relationship with enhanced vegetation index and meteorological parameters over South Asia.* Environmental Science and Pollution Research, vol. 29, 2020, pp. 30638–30655. https://doi.org/10.1007/s11356-021-17887-4.

[17] Wang W., He Q., Zhang M., Zhang W., Zhu H.: *Full-coverage 1-km estimates and spatiotemporal trends of aerosol optical depth over Taiwan from 2003 to 2019.* Atmospheric Pollution Research, vol. 13(11), 2022, 101579. https://doi.org/10.1016/j.apr.2022.101579.

[18] Khalid B., Khalid A., Muslim S., Habib A., Khan K., Alvim D.S., Shakoor S., Mustafa S., Zaheer S., Zoon M., Khan A.H., Ilyas S., Chen B.: *Estimation of aerosol optical depth in relation to meteorological parameters over eastern and western routes of China Pakistan economic corridor.* Journal of Environmental Sciences, vol. 99, pp. 28–39. https://doi.org/10.1016/j.jes.2020.04.045.

[19] Tan Y., Wang Q., Zhang Z.: *Assessing spatiotemporal variations of AOD in Japan based on Himawari-8 L3 V31 aerosol products: Validations and applications.* Atmospheric Pollution Research, vol. 13(6), 2022, 101439. https://doi.org/10.1016/j.apr.2022.101439.

[20] Luong N.D., Hieu B.T., Hiep N.H.: *Contrasting seasonal pattern between ground-based PM$_{2.5}$ and MODIS satellite-based aerosol optical depth (AOD) at an urban site in Hanoi, Vietnam.* Environmental Science and Pollution Research, vol. 29(6), 2022, pp. 41971–41982. https://doi.org/10.1007/s11356-021-16464-z.

[21] Abuelgasim A., Bilal M., Alfaki I.A.: *Spatiotemporal variations and long term trends analysis of aerosol optical depth over the United Arab Emirates*. Remote Sensing Applications: Society and Environment, vol. 23, 2021,100532. https://doi.org/10.1016/j.rsase.2021.100532.

[22] Yousefi R., Wang F., Ge Q., Shaheen A.: *Long term aerosol optical depth trend over Iran and identification of dominant aerosol types.* Science of The Total Environment, vol. 722, 2020, 137906. https://doi.org/10.1016/j.scitotenv.2020.137906.

[23] Gouda K.C., Gogeri I., Thippareddy A.S.: *Assessment of aerosol optical depth over Indian subcontinent during COVID-19 lockdown (March–May 2020).* Environment Monitoring and Assessment, vol. 194(3), 2022, 195. https://doi.org/10.1007/s10661-022-09855-3.

[24] Kumar A.: *Spatio-temporal variations in satellite based aerosol optical depths & aerosol index over Indian subcontinent: Impact of urbanization and climate change.* Urban Climate, vol. 32, 2020, 100598. https://doi.org/10.1016/j.uclim.2020.100598.

[25] Singh T., Ravindra K., Sreekanth V., Gupta P., Sembhi H., Tripathi S.N., Mor S.: *Climatological trends in satellite-derived aerosol optical depth over North India and its relationship with crop residue burning: Rural-urban contrast*. Science of the Total Environment, vol. 748, 2020, 140963. https://doi.org/10.1016/j.scitotenv.2020.140963.

[26] Gurjar B.R.: *Air pollution in India: Major issues and challenges*. MAGZTER: Energy Future, January – March 2021. https://www.magzter.com/stories/Education/Energy-Future/Air-Pollution-In-India-Major-Issues-And-Challenges [access: 5.04.2021].

[27] Census of India: *Registrar General and Census Commissioner of India*. 2011. https://censusindia.gov.in/census.website/ [access: 4.05.2019].

[28] Lyapustin A., Wang Y.: *MODIS Multi-Angle Implementation of Atmospheric Correction (MAIAC) Data User's Guide*. 2018. https://lpdaac.usgs.gov/documents/110/MCD19_User_Guide_V6.pdf [access: 1.06.2018].

[29] Ross M.S.: *Introductory Statistics*. 4th ed. Academic Press, London 2017.

[30] Sen P.K.: *Estimates of the regression coefficient based on Kendall's tau*. Journal of the American Statistical Association, vol. 63(324), 1968, pp. 1379–1389. https://doi.org/10.1080/01621459.1968.10480934.

[31] Yue S., Wang C.: *The Mann–Kendall test modified by effective sample size to detect trend in serially correlated hydrological series*. Water Resources Management, vol. 18(3), 2004, pp. 201–218. https://doi.org/10.1023/B:WARM.0000043140.61082.60.

[32] Hamed K.H., Rao A.R.: *A modified Mann–Kendall trend test for autocorrelated data.* Journal of Hydrology, vol. 204(1–4), pp. 182–196. https://doi.org/10.1016/S0022-1694(97)00125-X.

[33] Şen Z.: *Innovative trend analysis methodology*. Journal of Hydrologic Engineering, vol. 17(9), 2012, pp. 1042–1046. https://doi.org/10.1061/(ASCE)HE.1943-5584.0000556.

[34] Das J., Mandal T., Rahman A.T.M.S., Saha P.: *Spatio-temporal characterization of rainfall in Bangladesh: an innovative trend and discrete wavelet transformation approaches.* Theoretical and Applied Climatology, vol. 143(6), 2021, pp. 1557–1579. https://doi.org/10.1007/s00704-020-03508-6.

[35] Rousseau R., Egghe L., Guns R.: *Statistics.* [in:] Rousseau R., Egghe L., Guns R., *Becoming Metric-Wise: A Bibliometric Guide for Researchers*, Elsevier, 2008, pp. 67–97. https://doi.org/10.1016/B978-0-08-102474-4.00004-2.

[36] Lord D., Qin X., Geedipally S.R.: *Exploratory analyses of safety data.* [in:] Lord D., Qin X., Geedipally R., *Highway Safety Analytics and Modeling*, Elsevier, 2021, pp. 135–177. https://doi.org/10.1016/B978-0-12-816818-9.00015-9.

[37] Liu H., Chen C., Li Y., Duan Z., Li Y.: *Monitoring and spatial prediction of multidimensional air pollutants*. [in:] Liu H., Chen C., Li Y., Duan Z., Li Y., *Smart Metro Station Systems: Data Science and Engineering*, Elsevier, 2022, pp. 171–200. https://doi.org/10.1016/B978-0-323-90588-6.00007-X.

[38] Kharol S.K., Badarinath K.V.S., Sharma A.R., Kaskaoutis D.G., Kambe-zidis H.D.: *Multiyear analysis of Terra/Aqua MODIS aerosol optical depth and ground observations over tropical urban region of Hyderabad, India.* Atmospheric Environment, vol. 45(8), 2011, pp. 1532–1542. https://doi.org/10.1016/j.atmosenv.2010.12.047.

[39] David L.M., Ravishankara A.R., Kodros J.K., Venkataraman C., Sadavarte P., Pierce J.R.: *Aerosol optical depth over India.* Journal of Geophysical Research. Atmospheres, vol. 123(7), 2018, pp. 3688–3703. https://doi.org/10.1002%2F2017JD027719.

[40] Attri P., Sarkar S., Mani D.: *Classification and transformation of aerosols over selected Indian cities during reduced emissions under Covid-19 lockdown.* Journal of Earth System Science, vol. 131(3), 2022, 190. https://doi.org/10.1007/s12040-022-01916-y.

[41] Ramachandran S., Srivastava R., Sumita Kedia, Rajesh T.A.: *Contribution of natural and anthropogenic aerosols to optical properties and radiative effects over an urban location.* Environmental Research Letters, vol. 7(3), 2012, 034028. https://doi.org/10.1088/1748-9326/7/3/034028.

[42] Sinha P.R., Kaskaoutis D.G., Manchanda R.K., Sreenivasan S.: *Characteristics of aerosols over Hyderabad in southern Peninsular India: Synergy in classification techniques.* Annales Geophysicae, vol. 30(9), 2012, pp. 1393–1410. https://doi.org/10.5194/angeo-30-1393-2012.

[43] Badarinath K.V.S., Kharol S.K., Chand T.R.K., Parvathi Y.G., Anasuya T., Jyothsna A.N.: *Variations in black carbon aerosol, carbon monoxide and ozone over an urban area in Hyderabad, India during the forest fire season.* Atmospheric Research, vol. 85(1), 2007, pp. 18–26. https://doi.org/10.1016/j.atmosres.2006.10.004.